ELSEVIER

International Journal of Minerals, Metallurgy and Materials
Volume 16, Number 1, February 2009, Page 96

Materials

Fabrication and characterization of anodic oxide films on a Ti-10V-2Fe-3Al titanium alloy

Jian-hua Liu, Jun-lan Yi, Song-mei Li, Mei Yu, and Yong-zhen Xu

School of Materials Science and Engineering, Beihang University, Beijing 100191, China
(Received 2008-01-10)

Abstract: Anodic oxide films of the titanium alloy Ti-10V-2Fe-3Al in ammonium tartrate electrolyte without hydrofluoric acid or fluoride were fabricated. The morphology, components, and microstructure of the films were characterized by scanning electron microscopy (SEM), X-ray photoelectron spectroscopy (XPS), X-ray diffraction (XRD), and Raman spectroscopy. The results showed that the films were thick, uniform, and nontransparent. Such films exhibited sedimentary morphology, with a thickness of about 3 μm, and the pore diameters of the deposits ranged from several hundred nanometers to 1.5 μm. The films were mainly titanium dioxide. Some coke-like deposits, which may contain or be changed by OH, NH, C–C, C–O, and C=O groups, were doped in the films. The films were mainly amorphous with a small amount of anatase and rutile phase.

Key words: titanium alloys; anodic oxide films; titanium dioxide; pulse current method

1. Introduction

Titanium is a corrosion-resistant metal with applications in several fields, such as aerospace, chemical, and electrochemical industries [1-2]. It is also used for biomedical and dental implants [3-5]. The favorable corrosion resistance of titanium should be attributed to the anodic oxide film naturally formed on its surface [6]. Corrosion is believed to occur through "weak spots" in the natural oxide film; a forced increase in film thickness will eliminate such weak spots and increase the corrosion resistance. Anodic oxidation is a commonly used surface treatment on the titanium substrate to increase the thickness and the corrosion resistance of the film [7]. The properties of anodic oxide films strongly depend on their composition, structure, and thickness [8]. Therefore, several articles have been devoted to the studies of such characteristics of the films in different preparation conditions [9-11].

Ti-10V-2Fe-3Al is an excellent candidate for aerospace applications [1, 12] owing to its excellent properties. However, there are very few reports on the anodic oxide films of Ti-10V-2Fe-3Al [13].

Generally, the films are almost several tens of nanometers [14] to about 1 μm [15] in size. Such films are transparent and the colors of the films have been explained by the multiple-beam interference theory [16]. Jeong *et al*. [17] used hydrofluoric acid as the pretreatment reagent and prepared a 5-7-μm thick film at high voltage. Schmuki *et al*. [18-19] fabricated a thick anodic oxide film with the thickness of 2.5-7 μm, however, the electrolyte they used contained hydrofluoric acid [18] or fluoride [19]. Hydrofluoric acid and fluoride are harmful to the environment owing to their high toxicity and complexity of their disposal process.

A novel anodic oxidizing process on Ti-6Al-4V titanium alloys with Ce element was studied in the previous article [20]. In this article, the thick, uniform, and nontransparent anodic oxide films of titanium alloy Ti-10V-2Fe-3Al were fabricated in the ammonium tartrate electrolyte without hydrofluoric acid or fluoride. The morphology, components, and microstructure of the anodic oxide films were investigated by scanning electron microscopy (SEM), X-ray photoelectron spectroscopy (XPS), X-ray diffraction (XRD), and Raman spectroscopy.

2. Experimental

2.1. Fabrication of anodic oxide films

A Ti-10V-2Fe-3Al forged block was cut into the

Corresponding author: Jian-hua Liu, **E-mail:** liujh@buaa.edu.cn
Also available online at www.sciencedirect.com

sheets of 80 mm×25 mm×2 mm. The nominal composition (wt%) of Ti-10V-2Fe-3Al is V 10.100, Fe 20.100, Al 3.100, C <0.050, O <0.130, and Ti balanced. Each sample was abraded with the silicon carbide (SiC) paper of successive grades from 300 to 600 grit, followed by rinsing with acetone and deionized water successively and finally dried in air.

Anodic oxidation was carried out in a cell with a thermostat water bath and a magnetic stirring apparatus. The sample was used as the anode and a 1Cr18Ni9Ti stainless steel plate was used as the cathode in an electrolytic cell. The anode surface was less than 50% of that of the cathode. The electrolyte used was an aqueous solution of ammonium tartrate, which was prepared from analytical grade chemicals and deionized water. The sample suspended by a copper wire was partly immersed into the electrolyte, which ensured that the copper wire did not contact with the electrolyte. The area under the water was calculated before anodic oxidation for setting the current density.

Anodic oxidation was performed using a pulse galvanostatic power supply WMY-IV. The fabrication conditions were studied in detail previously [21]. The main parameters are shown in Table 1.

Table 1. Parameters of the fabrication process

Content of ammonium tartrate	3 g/L
Current density	10 A/dm^2
Duty ratio	30%
Frequency	100/min
Temperature	15±2°C
Agitation speed	100 r/min

2.2. Characterization of anodic oxide films

The sample morphology was observed by SEM (FEI-Quanta600D8032). The components of the sample surface were analyzed by XPS (Kratos-Axis Ultra, using Al K_α radiation at 225 W, 15 mA, 15 kV, C1s hydrocarbon peak at 284.80 eV). The microstructure of the anodic oxide films was determined by XRD (Rigaku-D/Max2200PC, using Cu K_α radiation at 40 kV, 40 mA, and at the scanning speed of 4°/min). Additional information was also obtained by Raman spectroscopy (Yvon Jobin Horiba-HR800, using a He-Ne laser without filter, 633 nm).

3. Results and discussion

3.1. Morphology of anodic oxide films

The films fabricated were uniform and nontransparent yellow. The sedimentary morphology of the anodic oxide films formed can be seen clearly in Fig. 1(a). The pores have diameters ranging from several hundred nanometers to 1.5 μm, and there are some particles on the surface. It is likely owing to the adsorption or deposition of some substances from the electrolyte, or to the fragments of the films. The ratiocination is demonstrated by the subsequent XPS results.

Fig. 1(b) shows a cross-sectional image of the anodic oxide film. The thickness of such a film is around 3 μm, which indicates that it is relatively thick, compared to the anodic oxide films fabricated on titanium and its alloys by other processes without hydrofluoric acid or fluoride.

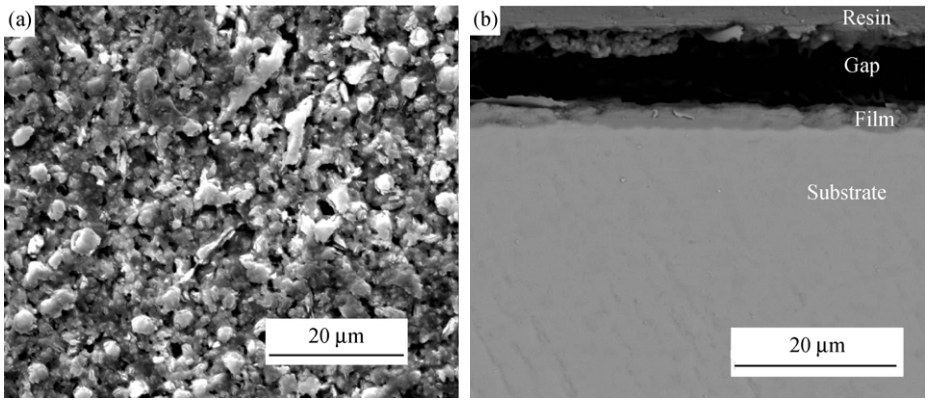

Fig. 1. Scanning electron images of the surface (a) and the cross-section (b) of anodic oxide films.

3.2. Components of anodic oxide films

The survey spectrum of anodic oxide films is presented in Fig. 2. It can be observed that the anodic oxide films mainly contain Ti, O, C, and N elements. The photoelectron peaks for Ti2p, O1s, C1s, and N1s appear clearly at the binding energies of 458.25, 530.01, 284.80, and 399.95 eV, respectively. The peak positions are in agreement with the reference values, which provide the O1s and Ti2p binding energies relative to the TiO_2 species of 530 and 458.6 eV, respectively [22].

Fig. 3 shows the high resolution XPS spectrum of the Ti2p region of anodic oxide films. The Ti2p photoemission signal splits in two peaks, the first at

the energy of 458.35 eV, attributed to $Ti2p_{3/2}$ (IV) at 458.8±0.1 eV, and the second at the energy of 464.04 eV, attributed to $Ti2p_{1/2}$ (IV) at 464.5±0.1 eV [8], showing that TiO_2 is the main constituent of the anodic oxide films.

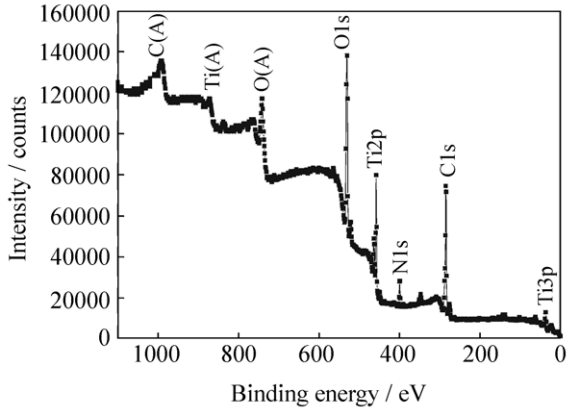

Fig. 2. XPS survey spectrum of anodic oxide films.

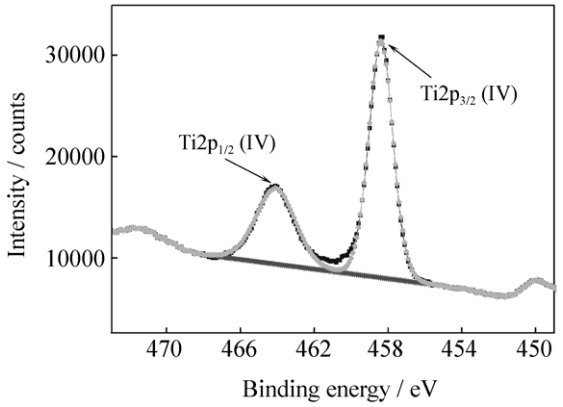

Fig. 3. XPS spectrum of the Ti2p region of anodic oxide films.

Fig. 4 shows the high resolution XPS spectrum of the O1s region of anodic oxide films. The O1s photoemission signal splits in three peaks, the first at the energy of 529.77 eV, attributed to Ti–O bonds at (530.5±0.2) eV, the second at the energy of 531.42 eV, attributed to OH bonds at (531.8±0.1) eV, and the third at the energy of 532.72 eV, attributed to adsorbed H_2O at (532.5±0.2) eV [8].

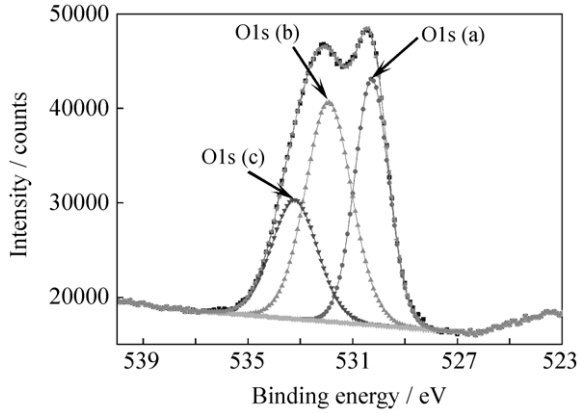

Fig. 4. XPS spectrum of the O1s region of anodic oxide films.

The high resolution XPS spectrum of the N1s region of anodic oxide films is shown in Fig. 5. The only peak is at 399.99 eV, which is attributed to the NH group [23], corresponding to the electrolyte.

Fig. 6 shows the high resolution XPS spectrum of the C1s region of anodic oxide films. Three peaks occur at 284.80, 286.28, and 288.07 eV for the prepared films. The first value arises from the adventitious elemental carbon (C–C), and the other two small peaks indicate the existence of C–O and C=O. This finding agrees well with the previous studies [24]. These groups are corresponding to the electrolyte. The molecular structural formula of ammonium tartrate is as follows.

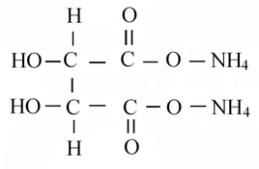

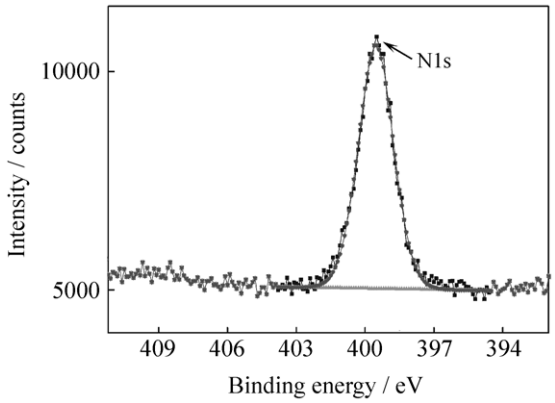

Fig. 5. XPS spectrum of the N1s region of anodic oxide films.

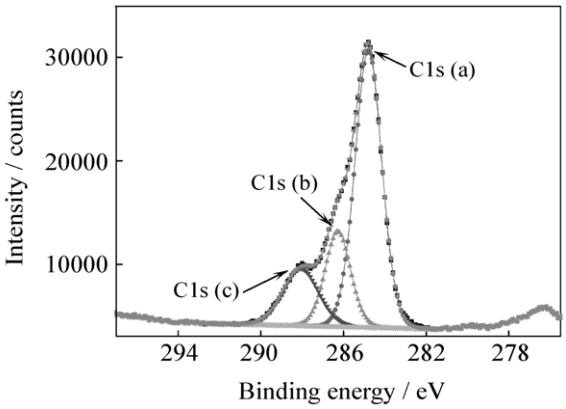

Fig. 6. XPS spectrum of the C1s region of anodic oxide films.

An ammonium tartrate molecule contains OH, NH, C–C, C–O, and C=O groups, which indicates that ammonium tartrate may absorb in the pores of the films and deposit after water volatilization, or be involved in the film formation reactions. The amount of carbon on the TiO_2 surface is responsible for good

visible-light absorbance. This may be attributed to the phenomenon that the film is nontransparent. A few oxygen atoms on the TiO_2 surface may be substituted by carbon to form a $TiO_{2-x}C_x$ structure. The XPS analysis of $Ti2p_{3/2}$ does not immediately reveal the Ti–C bond, and therefore, the $TiO_{2-x}C_x$ structure of these samples is probably scarce. Several OH groups transformed to highly condensed species, like coke, and were deposited and doped into anodic oxide films [25]. This is consistent with the ratiocination for the sedimentary morphology of anodic oxide films. Some sites are covered by coke species, causing an incomplete lattice structure (amorphous-like surface structure) on the anodic oxide films. Therefore, carbon in the films may play two roles: it is the sensitizer for visible-light absorption owing to its coke-like structure; it also exists as an impurity, which makes the lattice defect of TiO_2 form interface states that effectively lower the band gap.

3.3. Microstructure of anodic oxide films

Fig. 7 shows the XRD spectra of the anodic oxide films formed on Ti-10V-2Fe-3Al (a) and the oxide powder stripped from the Ti-10V-2Fe-3Al substrate (b). The peaks shown in Fig. 7(a) are related to the substrate. The typical small broad peak α in Fig. 7(b) indicates the presence of the amorphous structure [26]. The small broad peak α corresponding to the (101) peak 25.4° of anatase is observed, whereas the peak β refers to the (103) and (004) peaks of anatase. Peak χ is related to the (200) peak of anatase, and peak δ is associated with the (105) and (211) peaks of anatase [17]. The microstructure of the anodic oxide films in this article is different compared to that of the previous references owing to different compositions and thermal histories of the metallic substrate, electrolytes, and fabrication parameters. The crystal phase is not clearly seen in the spectra of the anodic films. Since (i) a relatively low temperature (15±2°C) cannot lead to amorphous to anatase and rutile crystal transformation, (ii) the alloying components of the Ti-10V-2Fe-3Al substrate inhibit the crystal nucleation, and (iii) the incorporation of ammonium and tartrate species into anodic oxide films is associated with the amorphous-to-crystalline transition, it is reasonable to conclude that such a low crystal composition in the anodic films is too small to be seen in the XRD spectra.

In order to obtain further information on the crystal structure on the surface of the films, the Raman spectrum of such films is shown in Fig. 8. In this spectrum, the two bands positioned at 380-450 and 600-650 cm^{-1} are corresponding to the characteristic peaks of anatase phase (E1g mode 399 cm^{-1}, Eg mode 640 cm^{-1}) and rutile phase (Eg mode 445 cm^{-1}, A1g mode 607 cm^{-1}). These bands were already observed in the suspension plasma sprayed TiO_2 coatings [27]. The appearance of the broad bands may be attributed to the effect of impurity doping, defects, and strains introduced from the pretreatment process [28]. The intense peak at 158 cm^{-1} is also corresponding to rutile (B1g mode 144 cm^{-1}) or anatase (Eg mode 147 cm^{-1}) [29]. This blue-shift peak of the anodic films is caused by a low degree of crystallization on the surface and small particles [25].

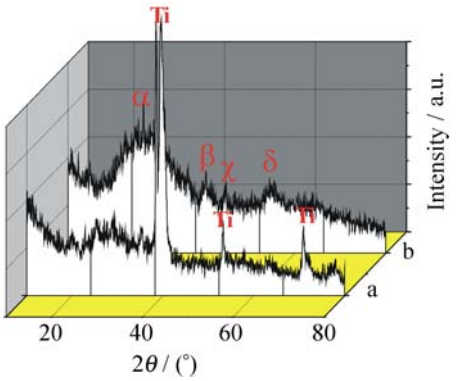

Fig. 7. X-ray spectra of the anodic oxide films (a) and the oxide powder (b).

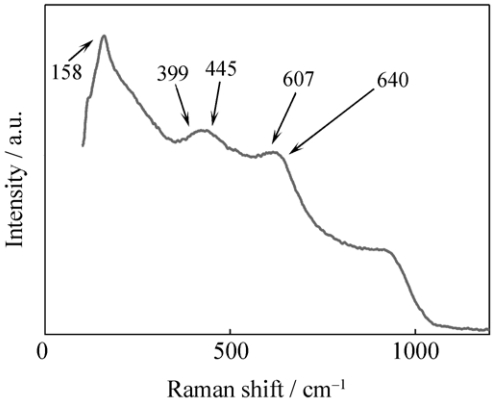

Fig. 8. Raman spectrum of anodic oxide films.

4. Conclusion

The thick, uniform, and nontransparent anodic oxide films of the titanium alloy Ti-10V-2Fe-3Al in ammonium tartrate electrolytes without toxic hydrofluoric acid and fluoride were successfully fabricated. The SEM results showed that some substances were adsorbed in or deposited on the films, exhibiting a sedimentary morphology with the film thickness of about 3 μm and pore diameters of the deposits ranging from several hundred nanometers to 1.5 μm. The XPS results showed that the films were mainly titanium dioxide. Some coke-like deposits, which may contain or be changed by OH, NH, C–C, C–O, and C=O groups, were doped in the films. The XRD results

showed that the films exhibited an amorphous structure with a small amount of anatase and rutile phase. The crystal phase was detected by Raman spectroscopy. Researches about the corrosion resistance of the films are in progress in our further study.

References

[1] R.R Boyer, An overview on the use of titanium in the aerospace industry, *Mater. Sci. Eng. A*, 213(1996), p.103.

[2] M.V. Popa, E. Vasilescu, P. Drob, M. Anghel, C. Vasilescu, I.M. Rosca, and A.S. Lopez, Anodic passivity of some titanium base alloys in aggressive environments, *Mater. Corros.*, 53(2002), p.51.

[3] J.C.M. Rosca, E.D.H. Santana, J.R. Castro, A.S. Lopez, E.V. Vasilescu, P. Drob, and C. Vasilescu, Characterization of anodic films formed on titanium and its alloys, *Mater. Corros.*, 56(2005), No.10, p.692.

[4] A.M. Al-Mayouf, A.A. Al-Swayih, and N.A. Al-Mobarak, Effect of potential on the corrosion behavior of a new titanium alloy for dental implant applications in fluoride media, *Mater. Corros.*, 55(2004), No.2, p.88.

[5] Z. Caia, T. Shafer, I. Watanabe, M.E. Nunn, and T. Okabe, Electrochemical characterization of cast titanium alloys, *Biomaterials*, 24(2003), p.213.

[6] Y. Fovet, J.Y. Gal, and F.T. Chemla, Influence of pH and fluoride concentration on titanium passivating layer stability of titanium dioxide, *Talanta*, 53(2001), p.1053.

[7] M.V. Diamanti and M.P. Pedeferri, Effect of anodic oxidation parameters on the titanium oxides formation, *Corros. Sci.*, 49(2007), p.939.

[8] J. Pouilleau, D. Devilliers, F. Garrido, S. Durand-Vidal, and E. Mahe. Structure and composition of passive titanium oxide films, *Mater. Sci. Eng. B*, 47(1997), p.235.

[9] C.E.B. Marino, E.M.D. Oliveira, R.C. RochaFilho, and S.R. Biaggio, On the stability of thin-anodic-oxide films of titanium in acid phosphoric media, *Corros. Sci.*, 43(2001), p.1465.

[10] S. Tanaka, N. Hirose, and T. Tanaki, Effect of the temperature and concentration of NaOH on the formation of porous TiO_2, *J. Electrochem. Soc.*, 152(2005), No.12, p.C789.

[11] V. Zwilling, M. Aucouturier, and E. Darque-Ceretti, Anodic oxidation of titanium and TA6V alloy in chromic media, An electrochemical approach, *Electrochim. Acta*, 45(1999), p.921.

[12] B. Wang, Z.Q. Liu, Y. Gao, S.Z. Zhang, and X.Y. Wang, Microstructural evolution during aging of Ti-10V-2Fe-3Al titanium alloy, *J. Univ. Sci. Technol. Beijing*, 14(2007), No.4, p.335.

[13] R.M. Peng, Fabrication method and performance for color inverted film of Ti-10V-2Fe-3Al alloy surface, *Hongdu Sci. Technol.* (in Chinese), 2(1999), p.24.

[14] Y.T. Sul, C.B. Johansson, Y. Jeong, and T. Albrektsson, The electrochemical oxide growth behavior on titanium in acid and alkaline electrolytes, *Med. Eng. Phys.*, 23(2001), p.329.

[15] Y.T. Sul, C.B. Johansson, S. Petronis, A. Krozer, Y. Jeong, A. Wennerberg, and T. Albrektsson, Characteristics of the surface oxides on turned and electrochemically oxidized pure titanium implants up to dielectric breakdown: the oxide thickness, micropore configurations, surface roughness, crystal structure and chemical composition, *Biomaterials*, 23(2002), p.491.

[16] J.L. Delplancke and R. Winand, Galvanostatic anodization of titanium-II reactions efficiencies and electrochemical behavior model, *Electrochim. Acta*, 33(1988), No.11, p.1551.

[17] X.L. Zhu, K.H. Kim, and Y. Jeong, Anodic oxide films containing Ca and P of titanium biomaterial, *Biomaterials*, 22(2001), p.2199.

[18] R. Beranek, H. Hildebrand, and P. Schmuki, Self-organized porous titanium oxide prepared in H_2SO_4/HF electrolytes, *Electrochem. Solid State Lett.*, 6(2003), No.3, p.B12.

[19] J.M. Macak, H. Tsuchiya, L. Taveira, S. Aldabergerova, and P. Schumuki, Smooth anodic TiO_2 nanotubes, *Angew. Chem. Int. Ed.*, 44(2005), p.7463.

[20] S.M. Li, H. Wu, J.H. Liu, and B.J. Wang, Study on effect of Ce on Ti-alloy anodization, *Acta Aeronaut. Astronaut. Sin.*, 23(2002), No.1, p.91.

[21] J.H. Liu, J.L. Yi, S.M. Li, G.R. Long, and W.K. Gan, *Anodic Oxidizing Process of Titanium Alloys in Ammonium Tartrate Electrolyte*, Chinese Patent, Appl.10088882.7, 2006.

[22] L. Wu, J.C. Yu, L.Z. Zhang, X.C. Wang, and W.K. Ho, Preparation of a highly active nanocrystalline TiO_2 photocatalyst from titanium oxo cluster precursor, *J. Solid State Chem.*, 177(2004), p.2584.

[23] W.S. Ma, X.R. Zeng, and K.C. Gong, Characterization of polyaniline/thiokol rubber composite film (II), *J. South China Univ. Technol. Nat. Sci.* (in Chinese), 27(1999), No.3, p.76.

[24] J. Xiang, S. Hu, L.S. Sun, M.H. Xu, P.S. Li, and X.X. Sun, Evolution of carbon and oxygen functional groups during coal combustion, *J. Chem. Ind. Eng.* (in Chinese), 57(2006), No.9, p.2180.

[25] C.S. Kuo, Y.H. Tseng , C.H. Huang, and Y.Y. Li, Carbon-containing nano-titania prepared by chemical vapor deposition and its visible-light-responsive photocatalytic activity, *J. Mol. Catal. A*, 270(2007), p.93.

[26] J.L. Delplanckle and R.Winand, Galvanostatic anodization of titanium-I. Structures and compositions of the anodic films, *Electrochim. Acta*, 33(1988), No.11, p.1539.

[27] R. Tomaszek, L. Pawlowski, L. Gengembre, J. Laureyns, and A.L. Maguer, Microstructure of suspension plasma sprayed multilayer coatings of hydroxyapatite and titanium oxide, *Surf. Coat. Technol.*, 201(2007), p.7432.

[28] J. Wang, Q.W. Zhang, S. Yin, T. Sato, and F. Saito, Raman spectroscopic analysis of sulphur-doped TiO_2 by co-grinding with TiS_2, *J. Phys. Chem. Solids*, 68(2007), p.189.

[29] X.Y. Pan and X.M. Ma, Progress of research on Raman spectra of nano-TiO_2, *Mater. Sci. Eng.* (in Chinese), 19(2001), No.4, p.138.